Article ID: 1006-8775(2012) 03-0393-10

RADIATIVE AND MICROPHYSICAL EFFECTS OF ICE CLOUDS ON A TORRENTIAL RAINFALL EVENT OVER HUNAN, CHINA

XU Feng-wen (许凤雯)[1], XU Xiao-feng (许小峰)[2], CUI Xiao-peng (崔晓鹏)[3], WANG Zhi (王　志)[1]

(1. Public Meteorological Service Centre of China Meteorological Administration, Beijing 100081 China; 2. China Meteorological Administration, Beijing 100081 China; 3. Laboratory of Cloud-Precipitation Physics and Severe Storms (LACS) of Institute of Atmospheric Physics, Beijing 100081 China)

Abstract: The radiative and microphysical effects of ice clouds on a torrential rainfall event over Hunan, China in June 2004 are investigated by analyzing the sensitivity of cloud-resolving model simulations. The model is initialized by zonally-uniform vertical velocity, zonal wind, horizontal temperature and vapor advection from National Centers for Environmental Prediction (NCEP) / National Center for Atmospheric Research (NCAR) reanalysis data. The exclusion of radiative effects of ice clouds increases model domain mean surface rain rates through the increase in the mean net condensation associated with the increase in the mean radiative cooling during the onset phase and the increases in the mean net condensation and the mean hydrometeor loss during the mature phase. The decrease in the mean rain rate corresponds to the decreased mean net condensation and associated mean latent heat release as the enhanced mean radiative cooling by the removal of radiative effects of ice clouds cools the mean local atmosphere during the decay phase. The removal of microphysical effects of ice clouds decreases the mean rain rates through the decrease in the mean net condensation during the onset phase, while the evolution of mean net condensation and the mean hydrometeor changes from decrease to increase during the mature phase. The reduction in the mean rain rate is primarily associated with the mean hydrometeor change in the absence of microphysical effects of ice clouds during the decay phase.

Key words: radiative and microphysical effects; ice clouds; rainfall; budget analysis; cloud-resolving model; simulation

CLC number: P435 **Document code:** A

1 INTRODUCTION

Torrential rainfall has profound socio-economic impacts on China and its accurate prediction relies on the improvement of understanding of rainfall processes[1]. There are many physical factors and processes affecting the development of precipitation. Among them, the development of convection and associated rainfall could be affected by the surface fluxes[2], wind shear[3], saturated environment, lower-tropospheric convergence[4], and ice microphysical processes[4-6]. The impacts of ice clouds on the development of convective systems have been intensively studied for decades using cloud-resolving model simulations[7-20]. Recently, Ping et al.[21] conducted a series of two-dimensional (2D) equilibrium cloud-resolving simulations imposed by zero large-scale vertical velocity and analyzed the simulation data with the diagnostic surface rainfall equation derived by Gao et al.[22]. They found that the exclusion of radiative effects of ice clouds increases the model domain mean surface rainfall by enhancing convective rainfall through the intensified water vapor convergence over convective regions. The exclusion of microphysical effects of ice clouds decreases the mean surface rainfall by reducing both convective and stratiform rainfall through weakening water vapor convergence over convective regions, and dries the air over stratiform rainfall regions and slows down the transport of hydrometeor concentration from convective to stratiform rainfall regions. Wang et al.[23] (hereafter W23) examined radiative and microphysical effects of ice clouds on a heavy rainfall event in the south of China in June 2008 and revealed that the exclusion of radiative effects of ice clouds decreases model domain mean rain rates during the onset and development phases whereas it increases them during the mature and decay phases. The exclusion of microphysical effects of ice clouds reduces the mean rain rates during the life span of the

Received 2011-01-18; **Revised** 2012-04-27; **Accepted** 2012-07-15
Foundation item: National Natural Science Foundation of China (40575029; 40775036; 40921160379)
Biography: XU Feng-wen, engineer, primarily undertaking research on cloud and precipitation physics.
Corresponding author: XU Feng-wen, e-mail: xuwen1996@163.com

rainfall event. The change in the mean rain rate, which results from the exclusion of radiative effects of ice clouds, and magnitude of the decrease in the mean rain rate, which results from the exclusion microphysical effects of ice clouds, depend on the large-scale forcing.

Xu et al.[24] carried out a 2D cloud-resolving simulation of a torrential rainfall event that occurred in Hunan, China in June 2004 and their analysis of the time- and domain-mean surface rainfall budget showed that water vapor convergence mainly supports local atmospheric moistening during the onset phase and surface rainfall during the mature stage. As a result, the surface rain rate is significantly smaller during the onset phase than during the mature phase. The weakened water vapor convergence finally reduces the surface rainfall during the decay phase. The comparison in imposed large-scale vertical velocity in Figure 1 shows similar vertical profiles of upward motions in this study and W23 during the onset phase, and weaker upward motions in this study than in W23 during the mature and decay phases. The vertical wind shears in this study are significantly larger during the onset and mature phases and are smaller during the decay phase than those in W23 (Figure 2). The different large-scale forcing may cause different radiative and microphysical effects of ice clouds on rainfall during the life of precipitation systems.

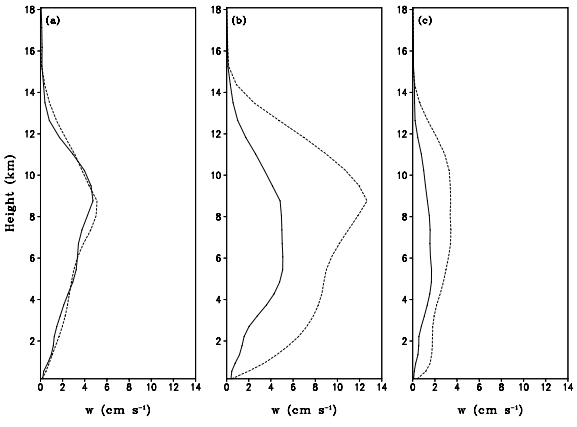

Figure 1. Vertical profiles of imposed large-scale vertical velocity (cm s^{-1}) averaged over (a) the onset phase, (b) the mature phase, and (c) the decay phase. The solid and dash lines denote the profiles in this study and Wang et al.[23], respectively.

In this study, the radiative and microphysical effects of ice clouds on a torrential rainfall event over Hunan, China in 2004 are examined by analyzing cloud-resolving model experiments. The model simulations are compared with the simulations conducted by W23 to examine the dependence of rainfall responses to radiative and microphysical effects of ice clouds on imposed large-scale upward motions. Since radiative processes of ice clouds directly affect the radiation term in heat budget and microphysical processes of ice clouds directly affect net latent heat in heat budget and net condensation and hydrometeor processes in cloud budget, heat and cloud budgets are first analyzed to highlight dominant physical processes that are responsible for radiative and microphysical effects of ice clouds on rainfall. Thus, the analysis is much more straightforward than the analysis in W23 in which the surface rainfall budget was first examined and followed by the analysis of heat budget. The model and experiments are briefly described in the next section. The results from the analysis of heat and cloud budgets are presented in section 3 and the results from the partitioning analysis of convective and stratiform rainfall based on surface rainfall budget are discussed in section 4. A summary is given in section 5.

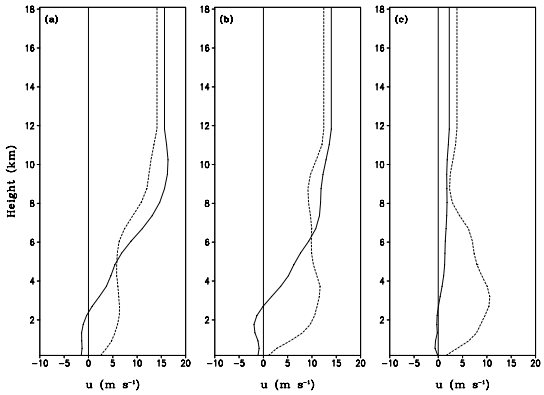

Figure 2. As in Figure 1 except for large-scale zonal wind (m s^{-1}).

2 MODEL AND EXPERIMENTS

The control experiment (CTRL) is designed based on the 2D version[24, 25] of cloud-resolving model[26-28] from Xu et al.[29], which was modified by Li et al.[16]. In Li et al.[16], the natural ice nucleus during the growth of cloud ice produced from sublimation in the scheme of Hsie et al.[30] is replaced with mean mass of ice crystal in Krueger et al.[31]. The mixing ratio, as shown in the calculation, is significantly increased. Moreover, the radius of the 50-μm ice crystal, based on in situ aircraft observations, increases from 50 (Hsie et al.[30]) to 100 μm (Krueger et al.[31]), as determined from calculation of the growth of snow due to the deposition and riming of cloud ice. The model includes prognostic equations for potential temperature, specific humidity, and perturbation momentum, and mixing ratios of cloud water, raindrops, cloud ice, snow, and graupel. The cloud microphysical parameterization schemes used in the model are developed by Rutledge and Hobbs[32, 33], Lin et al.[34], Tao et al.[35], and Krueger et al.[31]. The

model also includes solar[36] and thermal infrared[37, 38] radiation parameterization schemes that are performed every 3 minutes. The model uses cyclic lateral boundaries, a horizontal domain of 768 km, a horizontal grid resolution of 1.5 km, 33 vertical levels, and a time step of 12 s. A detailed model description can be found in Gao and Li[39]. The model is initialized by the zonally-uniform vertical velocity, zonal wind, and horizontal temperature and vapor advection from NCEP/NCAR reanalysis data (Figure 3) and is integrated from 0200 LST 23 June to 0200 LST 29 June 2004 (6 days in all). Xu et al.[24] conducted a comparison study between the observations and model simulations in terms of surface rain rate and radar reflectivity and showed that the simulated rain rate basically follows the evolution of observed rain rates.

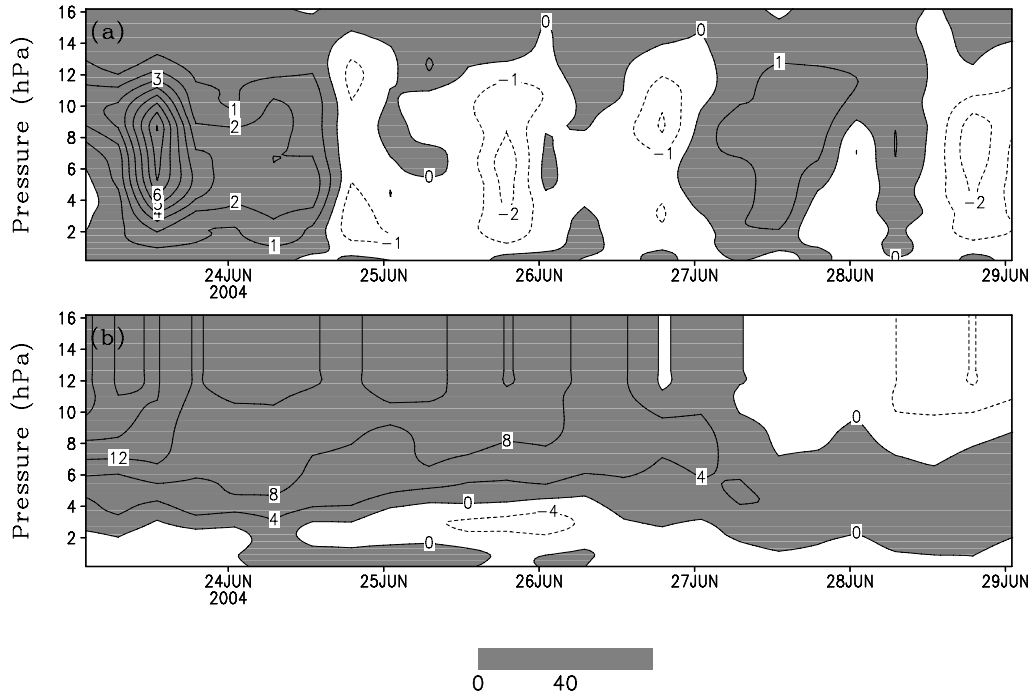

Figure 3. Time-height distribution of (a) vertical velocity (cm s^{-1}) and (b) zonal wind (m s^{-1}) from NCEP/NCAR reanalysis data. Upward motion in (a) and westerly wind in (b) are shaded.

Two additional sensitivity experiments are conducted in this study (Table 1). Experiments CNIR and CNIM are identical to CTRL except that the mixing ratios of ice hydrometeors are set to zero in the calculation of radiation in CNIR and the mixing ratios and associated microphysical rates of ice hydrometeors are set to zero in CNIM. The comparison between CNIR and CTRL (i.e., CNIR-CTRL) shows the responses of surface rainfall to the exclusion of radiative effects of ice clouds, whereas the comparison between CNIM and CNIR (i.e., CNIM-CNIR) reveals the responses of surface rainfall to the exclusion of microphysical effects of ice clouds in the absence of radiative effects of ice clouds. As shown in Xu et al.[24], the major rainfall process occurred during the 37-hour period from 0800 LST 23 June to 2000 LST 24 June 2004. Thus, the analysis is conducted in this study from 0800 LST to 1000 LST 23 June during the onset phase, from 1100 LST to 2100 LST 23 June during the mature phase, and from 2200 LST 23 June to 2000 LST 24 June 2004 during the decay phase.

Table 1. Experiment design.

Experiments	Radiation	Ice microphysics
CTRL	Yes	Yes
CNIR	No	Yes
CNIM	Yes	No

3 ANALYSIS OF MODEL DOMAIN MEAN BUDGETS

The radiative and microphysical effects of ice clouds affect radiation and latent heat in heat budget and net condensation in cloud budget. Thus, radiative and microphysical effects of ice clouds on model domain mean budget and clouds budgets are analyzed. Following Gao and Li[40], model domain mean heat budget can be expressed as:

$$S_{HT} + S_{HF} + S_{HS} + S_{LH} + S_{RAD} = 0, \quad (1)$$

where

$$S_{HT} = -\frac{\partial < \overline{T} >}{\partial t}, \quad (1a)$$

$$S_{HF} = - < \overline{u}^{o} \frac{\partial \overline{T}^{o}}{\partial x} > - < \pi \overline{w}^{o} \frac{\partial \overline{\theta}}{\partial z} >, \quad (1b)$$

$$S_{HS} = \overline{H}_s, \quad (1c)$$

$$S_{LH} = \frac{1}{c_p} < \overline{Q}_{cn} >, \quad (1d)$$

$$S_{RAD} = \frac{1}{c_p} < \overline{Q}_R >. \quad (1e)$$

Here, S_{HT}, S_{HF}, S_{HS}, S_{LH}, and S_{RAD} are local heat change, heat convergence, surface sensible heat, latent heat, and radiative heating, respectively; T and θ are air temperature and potential temperature, respectively, u and w are the zonal and vertical components of wind, respectively; c_p is the specific heat of dry air at constant pressure, H_s is surface sensible heat flux, Q_{cn} is the net latent heat through phase changes among water vapor, water hydrometeors, and ice hydrometeors [see (1.8a) in Gao and Li[39]], Q_R is the net radiative heating due to solar heating and infrared cooling, overbar is model domain mean, superscript "0" represents the NCEP/NCAR data, and $< () > (= \int_{z_b}^{z_t} \overline{\rho}() dz / \int_{z_b}^{z_t} \overline{\rho} dz)$ is mass-weighted mean, z_t and z_b are the heights of the top and bottom of the model atmosphere respectively.

To examine rainfall processes, the surface rainfall equation derived by Gao et al.[22] and Cui and Li[41] is adopted in this study, which can be written as:

$$P_s = Q_{WVT} + Q_{WVF} + Q_{WVE} + Q_{CM}, \quad (2)$$

where

$$Q_{WVT} = -\frac{\partial [q_v]}{\partial t}, \quad (2a)$$

$$Q_{WVF} = -[\overline{u}^{o} \frac{\partial \overline{q}_v^{o}}{\partial x}] - [\overline{w}^{o} \frac{\partial \overline{q}_v}{\partial z}] - [\frac{\partial (u' q_v')}{\partial x}]$$

$$-[\overline{u}^{o} \frac{\partial q_v'}{\partial x}] - [\overline{w}^{o} \frac{\partial q_v'}{\partial z}] - [w' \frac{\partial \overline{q}_v}{\partial z}], \quad (2b)$$

$$Q_{WVE} = E_s, \quad (2c)$$

$$Q_{CM} = -\frac{\partial [q_5]}{\partial t} - [\frac{\partial (u q_5)}{\partial x}]. \quad (2d)$$

Here, q_v is specific humidity, and E_s is surface evaporation rate. $q_5 = q_c + q_r + q_i + q_s + q_g$, q_c, q_r, q_i, q_s, q_g are the mixing ratios of cloud water, raindrops, cloud ice, snow, and graupel, respectively. $[()] = \int_{z_b}^{z_t} \overline{\rho}() dz$, which is a mass integration. Prime represents the perturbation from domain mean. Note that the surface rainfall equation was derived from the mass-integrated cloud budget,

$$P_s = Q_{CM} + Q_{NCS}, \quad (3)$$

and mass-integrated water vapor budget,

$$Q_{WVT} + Q_{WVF} + Q_{WVE} = Q_{NCS}. \quad (4)$$

Here $Q_{NCS} (= [P_{CND}] + [P_{DEP}] + [P_{SDEP}] + [P_{GDEP}] - [P_{REVP}] - [P_{MLTG}] - [P_{MLTS}])$ represents the net cloud condensation between vapor condensation ($[P_{CND}]$) and vapor deposition for the growth of cloud ice ($[P_{DEP}]$) and snow ($[P_{SDEP}]$) and graupel ($[P_{GDEP}]$) minus growth of vapor by evaporation of raindrop ($[P_{REVP}]$) and evaporation of liquid from graupel surface ($[P_{MLTG}]$), and evaporation of melting snow ($[P_{MLTS}]$).

Model domain mean heat budgets show that the exclusion of radiative effects of ice clouds enhances radiative cooling (S_{RAD}) from 0.029 °C h^{-1} in CTRL to –0.006 °C h^{-1} in CNIR during the onset period, from –0.007 °C h^{-1} in CTRL to –0.038 °C h^{-1} in CNIR during the mature period, and from –0.033 °C h^{-1} in CTRL to –0.051 °C h^{-1} in CNIR during the decay period (Table 2). During the onset period, the increases in the mean latent heat release ($S_{LH}>0$) and the associated mean net condensation ($Q_{NCS}>0$; Table 3) primarily correspond to the increase in the mean radiative cooling, while it is also related to the decrease in the mean local atmospheric cooling ($S_{HT}>0$). The mean cloud budget (Eq. 3) reveals that the increase in the mean net condensation is a primary contributor to the increase in the mean rain rate, whereas the decrease in the mean hydrometeor gain ($Q_{CM}<0$) also contributes to the increase in the mean rain rate. During the mature period, the enhanced mean latent heat and associated mean net condensation are mainly associated with the increase in the mean radiative cooling. The increase in the mean rain rate corresponds to the increases in the mean net condensation and mean hydrometeor loss ($Q_{CM}>0$). During the decay period, the increase in the mean radiative cooling is used to cool the mean local atmosphere while the mean latent heat and associated mean net condensation are decreased. As a result, the decrease in the mean rain rate is related to the decrease in the mean net condensation.

Table 2. Model domain means of heat budget [radiative heating (SRAD), local heat change (SHT), heat convergence (SHF), surface sensible flux (SHS), and latent heat (SLH)] in the control experiment (CTRL), the experiment with the exclusion of ice radiative effects (CNIR), and the experiment with the total exclusion of ice microphysics (CNIM) and their differences for CNIR-CTRL and CNIM-CNIR averaged from 0800 LST to 1000 LST 23 June during the onset period in (a), from 1100 LST to 2100 LST 23 June during the mature period in (b), and from 2200 LST 23 June to 2000 LST 24 June 2004 during the decay period in (c). Units: °C h^{-1}.

(a)	CTRL	CNIR	CNIM	CNIR-CTRL	CNIM-CNIR
S_{RAD}	0.029	–0.006	0.007	–0.035	0.013
S_{HT}	0.116	0.076	0.123	–0.040	0.047
S_{HF}	–0.280	–0.277	–0.267	0.003	0.010
S_{HS}	0.000	0.001	0.000	0.001	–0.001
S_{LH}	0.134	0.206	0.137	0.072	–0.069

(b)	CTRL	CNIR	CNIM	CNIR-CTRL	CNIM-CNIR
S_{RAD}	–0.007	–0.038	–0.023	–0.031	0.015
S_{HT}	0.004	–0.009	0.024	–0.013	0.033
S_{HF}	–0.449	–0.442	–0.428	0.007	0.014
S_{HS}	0.004	0.004	0.004	0.000	0.000
S_{LH}	0.448	0.485	0.423	0.037	–0.062

(c)	CTRL	CNIR	CNIM	CNIR-CTRL	CNIM-CNIR
SRAD	–0.033	–0.051	–0.036	–0.018	0.015
SHT	0.029	0.052	0.037	0.023	–0.015
SHF	–0.144	–0.140	–0.138	0.004	0.002
SHS	0.006	0.006	0.005	0.000	–0.001
SLH	0.142	0.132	0.132	–0.010	0.000

Table 3. Model domain means of cloud budget [surface rain rate (P_S), hydrometeor change/convergence (Q_{CM}), and net cloud source Q_{NCS}] in the control experiment (CTRL), the experiment with the exclusion of ice radiative effects (CNIR), and the experiment with the total exclusion of ice microphysics (CNIM) and their differences for CNIR-CTRL and CNIM-CNIR averaged from 0800 LST to 1000 LST 23 June during the onset period in (a), from 1100 LST to 2100 LST 23 June during the mature period in (b), and from 2200 LST 23 June to 2000 LST 24 June 2004 during the decay period in (c). Units: mm h^{-1}.

(a)	CTRL	CNIR	CNIM	CNIR-CTRL	CNIM-CNIR
P_S	0.417	0.765	0.300	0.348	–0.465
Q_{CM}	–0.286	–0.195	–0.302	0.091	–0.107
Q_{NCS}	0.703	0.960	0.602	0.257	–0.358

(b)	CTRL	CNIR	CNIM	CNIR-CTRL	CNIM-CNIR
P_S	1.739	1.896	1.571	0.157	–0.325
Q_{CM}	0.031	0.101	–0.053	0.070	–0.154
Q_{NCS}	1.708	1.795	1.624	0.087	–0.171

(c)	CTRL	CNIR	CNIM	CNIR-CTRL	CNIM-CNIR
P_S	0.570	0.535	0.460	–0.035	–0.075
Q_{CM}	0.040	0.040	–0.021	0.000	–0.061
Q_{NCS}	0.530	0.495	0.481	–0.035	–0.014

The exclusion of ice clouds reduces the mean net condensation through the removal of vapor deposition to ice hydrometeors during the life span of a precipitation system, as indicated in Table 3, in which the mean net condensation rates are lower in CNIM than in CTRL. The mean cloud budgets (Table 4) show that the decrease in the mean rain rate is associated with the decrease in the mean net condensation during the life span of a precipitation system, while it is also related to the mean hydrometeor change from “loss” in CTRL to “gain” in CNIM during the mature and decay periods. Thus, the exclusion of radiative effects of ice clouds (CNIR-CTRL) increases the mean rain rate through the enhanced mean latent heat release associated with the enhanced mean radiative cooling and the exclusion of microphysical effects of ice clouds (CNIM-CNIR) reduces the mean rain rate through the decrease in the mean net condensation associated with the removal of vapor deposition.

During the onset phases, the exclusion of radiative effects of ice clouds increases the mean latent heating rate in this study, whereas it barely changes the mean latent heating rate in W23 (see their Table 3a). In this study, the removal of radiative effects of ice clouds change the mean radiation to

cooling in CNIR from heating in CTRL, while it enhances the mean radiative cooling from CTRL to CNIR. As a result, the difference in the mean radiative cooling rate is much lower in W23 than in this study. The increase in the mean latent heating corresponds to the change in the mean radiation from heating in CTRL to cooling in CNIR, which leads to the decrease in the mean local atmospheric cooling in this study. In contrast, the increase in the mean local atmospheric cooling corresponds to the increase in the mean radiative cooling in W23. The increase in the mean rain rate resulting from the exclusion of radiative effects of ice clouds is primarily related to the increase in the mean net condensation associated with the increase in the mean latent heat in this study, but the decrease in the mean rain rate is primarily associated with the slowdown in the mean hydrometeor loss in W23 (see their Table 2a). The decrease in the mean rain rate resulting from the exclusion of microphysical effects of ice clouds is primarily related to the decrease in the net condensation in this study, but the decrease in the mean rain rate is associated with the mean hydrometeor change from decrease to increase in W23.

Table 4. Fractional coverage (%) of (a) convective and (b) stratiform rainfall in the control experiment (CTRL), the experiment with the exclusion of ice radiative effects (CNIR), and the experiment with the total exclusion of ice microphysics (CNIM) and their differences for CNIR-CTRL and CNIM-CNIR averaged from 0800 LST to 1000 LST 23 June during the onset period, from 1100 LST to 2100 LST 23 June during the mature period, and from 2200 LST 23 June to 2000 LST 24 June 2004 during the decay period.

(a)	CTRL	CNIR	CNIM	CNIR-CTRL	CNIM-CNIR
Onset	23.6	16.7	44.7	–6.9	28.0
Mature	17.0	17.0	35.3	0.0	18.3
Decay	30.1	23.3	37.1	–6.8	13.8

(b)	CTRL	CNIR	CNIM	CNIR-CTRL	CNIM-CNIR
Onset	73.8	77.9	26.9	4.1	–51.0
Mature	75.3	63.8	32.2	–11.5	–31.6
Decay	57.6	54.6	40.8	–3.0	–13.8

During the mature phase, the exclusion of radiative (microphysical) effects of ice clouds increases (decreases) the mean latent heating rates and the mean surface rain rate. Further analysis of cloud budgets reveals that the increase in the mean rain rate resulting from the exclusion of radiative effects of ice clouds is related to the increase in the mean latent heat and the hydrometeor loss in this study, but it is primarily associated with the increase in the mean hydrometeor loss in W23 (see their Table 2c). The decrease in the mean rain rate is related to the decrease in the mean net condensation and the mean hydrometeor change from decrease to increase through the growth of cloud water in this study, Ping et al.[21] and W23.

During the decay phase, the removal of radiative effects of ice clouds slightly decreases the mean latent heating rate and the removal of microphysical effects of ice clouds barely changes the mean latent heating rate and slightly decreases the mean net condensation in this study. Moreover, the decrease in the mean rain rate resulting from the exclusion of radiative effects of ice clouds is related to the decrease in the mean net condensation associated with the decrease in the mean latent heat. However, the decrease in the mean rain rate resulting from the exclusion of microphysical effects of ice clouds is primarily associated with the mean hydrometeor change from decrease to increase. The elimination of radiative and microphysical effects of ice clouds increases the mean latent heating rate in W23) (see their Table 3d). The increase in the mean rain rate resulting from the removal of radiative effects of ice clouds is primarily related to the increase in the mean net condensation associated with the increase in the mean latent heat. In comparison, the decrease in the mean rain rate resulting from the exclusion of microphysical effects of ice clouds is associated with the mean hydrometeor change from decrease to increase.

4 ANALYSIS OF CONVECTIVE AND STRATIFORM RAINFALL

Surface rainfall includes convective and stratiform rainfall types. The major differences between convective and stratiform rainfall are: (1) the convective rain rate is usually higher than the stratiform rain rate; (2) horizontal reflectivity gradients and upward motions associated with convective rainfall are much stronger than those associated with stratiform rainfall; (3) the accretion of cloud water by raindrops via collisions in strong updraft cores and the vapor deposition on ice particles are primary microphysical processes associated with convective and stratiform rainfall, respectively[42]. To study convective and stratiform rainfall separately, the grid data are partitioned for the two categories. Many previous studies have performed convective/stratiform cloud partitioning based on the amplitude and spatial variations of radar reflectivity or surface rainfall rate[43-45]. Additional information like cloud contents, vertical motion, and the fall speed of precipitation

particles is also used in partitioning methods[10, 27, 28, 46-48]. The partitioning method proposed by Sui et al.[28] is used in this study. Sui et al.[28] identified model grid point as convective if the rain rate at this grid point is twice as large as the average taken over the surrounding four grid points (two grid points on either side of this grid point in a two-dimensional framework) or the rain rate at this grid point is greater than 20 mm h^{-1}. All non-convective cloudy grid points are considered as stratiform. The grid points in the stratiform regions are further checked and classified as convective if they are in the precipitating stratiform regions and cloud water mixing ratio below the melting level is larger than 0.5 g kg^{-1} or the maximum updraft above 600 hPa exceeds 5 m s^{-1}, or, if they are in the non-precipitating stratiform regions where cloud water mixing ratio is larger than 0.025 g kg^{-1} or the maximum updraft exceeds 5 m s^{-1} below the melting level.

During the onset phase, the exclusion of radiative effects of ice clouds decreases the fractional coverage of convective rainfall whereas it increases the fractional coverage of stratiform rainfall (Table 4). Both convective and stratiform rain rates are increased. The increase in convective rainfall is associated with the decreases in local atmospheric moistening and hydrometeor gain/divergence (Figure 4) and the increase in stratiform rainfall is related to the intensification in water vapor convergence over stratiform rainfall regions (Figure 5). The removal of microphysical effects of ice clouds significantly increases the fractional coverage of convective rainfall but it severely destroys stratiform clouds and shrinks the fractional coverage of stratiform rainfall. Both convective and stratiform rainfall are decreased due to the accelerations in local atmospheric drying and hydrometeor gain/divergence over convective regions and the slowdown in water vapor convergence over stratiform rainfall regions.

During the mature phase, the elimination of radiative effects of ice clouds barely changes the fractional coverage of convective rainfall but it decreases the fractional coverage of stratiform rainfall (Table 4). The exclusion of both radiative and microphysical effects of ice clouds increases convective rainfall (Figure 4) whereas it decreases stratiform rainfall (Figure 5). The increases in convective rainfall caused by the exclusion of radiative and microphysical effects of ice clouds have similar magnitudes whereas the decrease in stratiform rainfall caused by the exclusion of microphysical effects of ice clouds is much larger than that caused by the exclusion of radiative effects of ice clouds. The increases in convective rainfall are primarily associated with the enhancement in water vapor convergence over convective regions. In comparison, the decreases in stratiform rainfall are primarily related to the slowdowns in water vapor convergence over stratiform rainfall regions. The decrease in hydrometeor loss/convergence also contributes to the decrease in stratiform rainfall due to the exclusion of microphysical effects of ice clouds.

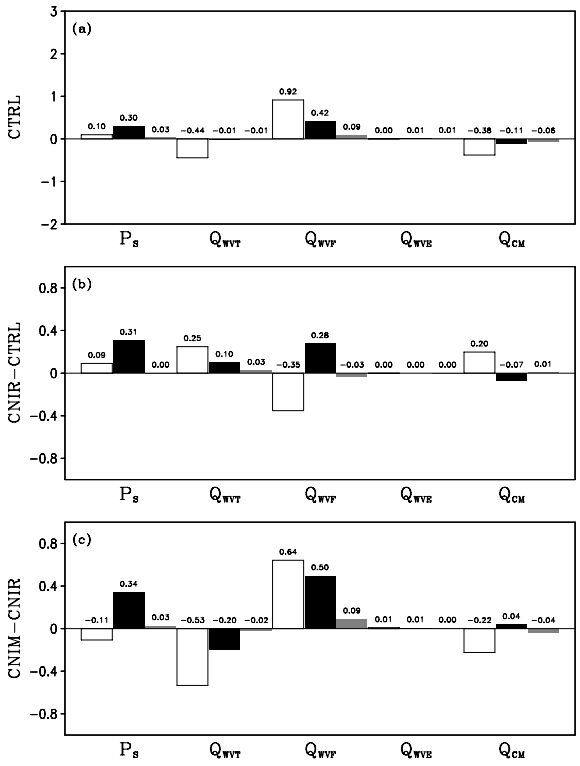

Figure 4. Surface rain rate (Ps), local water vapor change (Q_{WVT}), water vapor convergence (Q_{WVF}), surface evaporation (Q_{WVE}), and local hydrometeor change/hydrometeor convergence (Q_{CM}) over convective regions in the (a) control experiment (CTRL), and their difference fields for (b) CNIR-CTRL and (c) CNIM-CNIR averaged from 0800 LST to 1000 LST 23 June during the onset period (open bar), from 1100 LST to 2100 LST 23 June during the mature period (black bar), and from 2200 LST 23 June to 2000 LST 24 June 2004 during the decay period (grey bar). Units: mm h^{-1}.

During the decay phase, the exclusion of radiative effects of ice clouds decreases the fractional coverage of convective and stratiform rainfall (Table 4). The exclusion of microphysical effects of ice clouds increases the fractional coverage of convective rainfall while it decreases the fractional coverage of stratiform rainfall. The convective rainfall is insensitive to the radiative effects of ice clouds because of the large offset between the decrease in water vapor convergence and the local atmospheric change from moistening in CTRL to drying in CNIR (Figure 4). The stratiform rainfall is decreased by the exclusion of radiative effects of ice clouds through the slowdown in local atmospheric drying over raining stratiform regions (Figure 5). The removal of microphysical effects of ice clouds enhances convective rainfall though the intensification in water vapor convergence over convective regions, whereas

it decreases stratiform rainfall by cutting water vapor convergence and suppressing hydrometeor loss/convergence over stratiform raining regions.

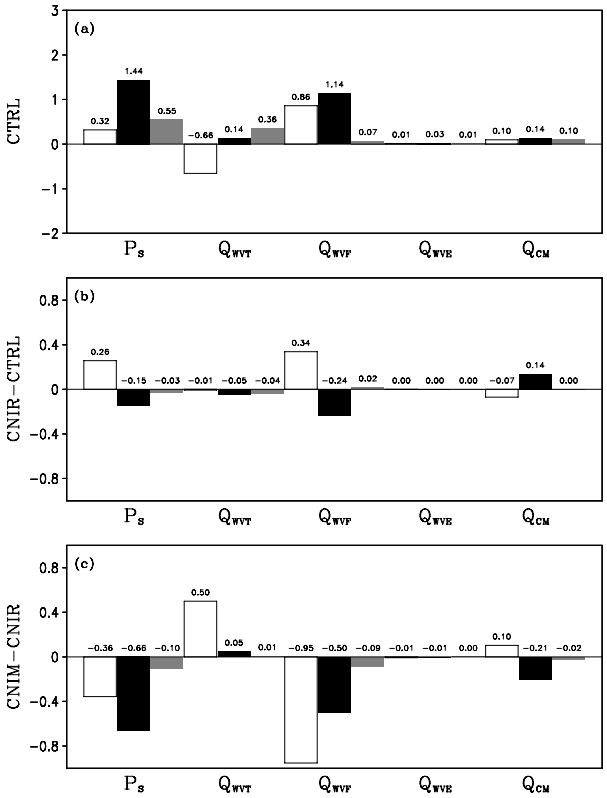

Figure 5. As in Figure 4, except for stratiform rainfall regions.

5 SUMMARY

The radiative and microphysical effects of ice clouds on the torrential rainfall event that occurred in Hunan, China in June 2004 are investigated using two-dimensional cloud-resolving model simulations. All experiments are initialized with zonally-uniform vertical velocity, zonal wind, horizontal temperature and vapor advection from NCEP/NCAR reanalysis data. The analysis of model domain mean budgets shows that the exclusion of radiative effects of ice clouds leads to the change from radiative heating to radiative cooling during the onset phase and the intensification in radiative cooling during the mature phase, which are mainly balanced by the increase in latent heat. The enhancement in the mean net condensation is associated with the increase in the mean latent heat, which causes the increase in the mean surface rainfall during the onset and mature phases. The exclusion of microphysical effects of ice clouds directly reduces the mean rainfall through the decreases in the mean net condensation and mean latent heat during the onset and mature phases. During the decay phase, the increase in the mean radiative cooling, which is caused by the exclusion of radiative effects of ice clouds, and the reduction in the mean latent heat and net condensation, which is caused by the exclusion of microphysical effects of ice clouds, are not directly responsible for the decreased mean rainfall. Instead, the reduction in the mean surface rainfall is related to the decrease in the mean net condensation and associated mean latent heat release, as the increase in the mean radiative cooling is used to cool the mean local atmosphere, which also results in the mean hydrometeor change from loss to gain, as the removal of microphysical effects of ice clouds slightly decreases the mean net condensation.

The partitioning analysis reveals that decreases in the mean surface rainfall caused by the exclusion of the microphysical effects of ice clouds is associated with the decreases in stratiform rainfall through the slowdowns in water vapor convergence over stratiform rainfall regions during the life cycle of a rainfall event. The increases in the mean surface rainfall caused by the exclusion of radiative effects of ice clouds are related to the stratiform rainfall strengthened by the enhanced water vapor convergence over stratiform rainfall regions during the onset phase, and to the convective rainfall intensified through the increased water vapor convergence over convective regions during the mature phase. In comparison, the decrease in the mean surface rainfall by the exclusion of radiative effects of ice clouds during the decay phase comes from the slowdown in stratiform rainfall through the weakened local atmospheric drying effect.

Further examination of three dimensional cloud-resolving model simulations is necessary in our next study to validate radiative and microphysical effects of ice clouds on rainfall from the two-dimensional model simulations in this study

Acknowledgement: The authors thank Dr. W.-K. Tao at NASA/GSFC for sharing the cloud-resolving model, Prof. SHEN Xin-yong at the Nanjing University of Information Science and Technology for providing simulation data, and three anonymous reviewers for valuable comments.

REFERENCES:

[1] HU Zhi-jin, ZOU Guang-yuan. Non-hydrostatic atmospheric numerical model and elastic adaptation process [J]. Sci. China (Ser. B), 1991, 21(5): 550-560.

[2] KONG Fan-you, HUANG Mei-yuan, XU Hua-ying. The effects of cold water surface on cumulus clouds: A numerical experiment [J]. Chin. J. Atmos. Sci., 1987, 11(2): 160-166.

[3] XU Hua-ying, JI Wu-sheng, HUANG Mei-yuan. A numerical study of the effects of wind shear on convective development [J]. Chin. J. Atmos. Sci., 1988, 12(4): 405-411.

[4] HONG Yan-chao. The numerical simulation study of convective-stratiform mixed cloud, part Ⅱ: Interaction of clouds and formative mechanism of the heavy rain [J]. Acta. Meteor. Sin., 1996, 54(6): 661-674 (in Chinese).

[5] KONG F, HUANG M, XU H. A three-dimensional numerical study of the effects of ice microphysics on the development of convective clouds [J]. Sci. China (Ser. B), 1991,

21(9): 1000-1008.
[6] YANG Jing, WANG Peng-yun, LI Xing-rong. Meso-scale simulation of cloud and precipitation physical processes in Mei-yu front system in June, 1999 [J]. J. Trop. Meteor., 2003, 19(2): 203-212.
[7] YOSHIZAKI M. Numerical simulations of tropical squall-line clusters: Two-dimensional model [J]. J. Meteor. Soc. Japan, 1986, 64(4): 469-491.
[8] NICHOLLS M E. A comparison of the results of a two-dimensional numerical simulation of a tropical squall line with observations [J]. Mon. Wea. Rev., 1987, 115(12): 3055-3077.
[9] FOVELL R G, OGURA Y. Numerical simulation of a midlatitude squall line in two dimensions [J]. J. Atmos. Sci., 1988, 45(24): 3846-3879.
[10] TAO W, SIMPSON J. Modeling study of a tropical squall-type convective line [J]. J. Atmos. Sci., 1989, 46(2): 177-202.
[11] MCCUMBER M, TAO W, SIMPSON J, et al. Comparison of ice-phase microphysical parameterization schemes using numerical simulations of tropical convection [J]. J. Appl. Meteor., 1991, 30(7): 985-1004.
[12] TAO W, SIMPSON J, SOONG S. Numerical simulation of a subtropical squall line over the Taiwan Strait [J]. Mon. Wea. Rev., 1991, 119(11): 2699-2723.
[13] LIU C, MONCRIEFF M W, ZIPSER E J. Dynamic influence of microphysics in tropical squall lines: A numerical study [J]. Mon. Wea. Rev., 1997, 125(9): 2193-2210.
[14] GRABOWSKI W, WU X, MONCRIEFF M. Cloud-resolving model of tropical cloud systems during Phase III of GATE. Part III: Effects of cloud microphysics [J]. J. Atmos. Sci., 1999, 56(14): 2384-2402.
[15] WU X, HALL W, GRABOWSKI W, et al. Long-term behavior of cloud systems in TOGA COARE and their interactions with radiative and surface processes. Part II: Effects of ice microphysics on cloud-radiation interaction [J]. J. Atmos. Sci., 1999, 56(18): 3177-3195.
[16] LI X, SUI C, LAU K, et al. Large-scale forcing and cloud-radiation interaction in the tropical deep convective regime [J]. J. Atmos. Sci., 1999, 56(17): 3028-3042.
[17] GRABOWSKI W, MONCRIEFF M. Large-scale organization of tropical convection in two-dimensional explicit numerical simulations [J]. Quart. J. Roy. Meteor. Soc., 2001, 127(572): 445-468.
[18] WU X. Effects of ice microphysics on tropical radiative-convective-oceanic quasi-equilibrium states [J]. J. Atmos. Sci., 2002, 59(11): 1885-1897.
[19] GRABOWSKI W. Impact of ice microphysics on multiscale organization of tropical convection in two-dimensional cloud-resolving simulations [J]. Quart. J. Roy. Meteor. Soc., 2003, 129(587): 67-81.
[20] GAO S, RAN L, LI X. Impacts of ice microphysics on rainfall and thermodynamic processes in the tropical deep convective regime: A 2D cloud-resolving modeling study [J]. Mon. Wea. Rev., 2006, 134(10): 3015-3024.
[21] PING F, LUO Z, LI X. Microphysical and radiative effects of ice microphysics on tropical equilibrium states: A two-dimensional cloud-resolving modeling study [J]. Mon. Wea. Rev., 2007, 135(7): 2794-2802.
[22] GAO S, CUI X, ZHU Y, et al. Surface rainfall processes as simulated in a cloud resolving model [J], J. Geophys. Res., 2005, 110(D10202), doi: 10.1029/2004JD005467.
[23] WANG Y, SHEN X, LI X. Microphysical and radiative effects of ice clouds on responses of rainfall to the large-scale forcing during pre-summer heavy rainfall over southern China [J]. Atmos. Res., 2010, 97(1-2): 35-46.
[24] SUI C H, LAU K, TAO W, et al. The tropical water and energy cycles in a cumulus ensemble model Part I: Equilibrium climate [J]. J. Atmos. Sci., 1994, 51(5): 711-728.
[25] SUI C, LI X, LAU K, Radiative-convective processes in simulated diurnal variations of tropical oceanic convection [J]. 1998, J. Atmos. Sci., 55(13): 2345-2359.
[26] SOONG S T, OGURA Y. Response of tradewind cumuli to large-scale processes [J]. J. Atmos. Sci., 1980, 37(9): 2035-2050.
[27] SOONG S, TAO W. Response of deep tropical cumulus clouds to mesoscale processes [J]. J. Atmos. Sci., 1980, 37(9): 2016-2034.
[28] TAO W, SIMPSON J. The Goddard Cumulus Ensemble model. Part I: Model description [J]. Terr. Atmos. Oceanic Sci., 1993, 4(1): 35-72.
[29] XU X, XU F, LI B. A cloud-resolving modeling study of a torrential rainfall event over China [J]. J. Geophys. Res., 2007, 112(D17204): doi: 10.1029/2006JD008275.
[30] HSIE E, FARLEY R, ORVILLE H. Numerical simulation of ice-phase convective seeding [J]. J. Appl. Meteor., 1980, 19(8): 950-977.
[31] KRUEGER S, FU Q, LIOU K, et al. Improvement of an ice-phase microphysics parameterization for use in numerical simulations of tropical convection [J]. J. Appl. Meteor., 1995, 34(1): 281-287.
[32] RUTLEDGE S, HOBBS P. The mesoscale and microscale structure and organization of clouds and precipitation in midlatitude cyclones. Part VIII: A model for the "seeder-feeder" process in warm-frontal rainbands [J]. J. Atmos. Sci., 1983, 40(5):1185-1206.
[33] RUTLEDGE S, HOBBS P. The mesoscale and microscale structure and organization of clouds and precipitation in midlatitude cyclones. Part XII: A diagnostic modeling study of precipitation development in narrow cold-frontal rainbands [J]. J. Atmos. Sci., 1984, 41(20): 2949-2972.
[34] LIN Y, FARLEY R, ORVILLE H. Bulk parameterization of the snow field in a cloud model [J]. J. Climate Appl. Meteor., 1983, 22(6): 1065-1092.
[35] TAO W, SIMPSON J, MCCUMBER M. An ice-water saturation adjustment [J]. Mon. Wea. Rev., 1989, 117(1): 231-235.
[36] CHOU M, SUAREZ M, HO C, et al. Parameterizations for cloud overlapping and shortwave single scattering properties for use in general circulation and cloud ensemble models [J]. J. Climate, 1998, 11(2): 202-214.
[37] CHOU M, KRATZ D, RIDGWAY W. Infrared radiation parameterization in numerical climate models [J]. J. Climate, 1991, 4(4): 424-437.
[38] CHOU M D, SUAREZ M J. An efficient thermal infrared radiation parameterization for use in general circulation model [R]. NASA Tech. Memo., 1994, 104606, Vol.3, 85pp.
[39] GAO S, LI X. Cloud-resolving modeling of convective processes [M]. Dordrecht: Springer, 2008, 206pp.
[40] GAO S, LI X. Responses of tropical deep convective precipitation systems and their associated convective and stratiform regions to the large-scale forcing [J]. Quart. J. Roy. Meteor. Soc., 2008, 134(637): 2127-2141.
[41] CUI X, LI X. Role of surface evaporation in surface rainfall processes [J]. J. Geophys. Res., 2006, 111(D17112): doi: 10.1029/2005JD006876.
[42] HOUGHTON H G.. On precipitation mechanisms and their artificial modification [J]. J. Appl. Meteor., 1968, 7(5): 851-859.
[43] CHURCHILL D D, HOUZE R A (Jr.). Development and structure of winter monsoon cloud clusters on 10 December 1978 [J]. J. Atmos. Sci., 1984, 41(6): 933-960.

[44] CANIAUX G, REDELSPERGER J L, LAFORE J P. A numerical study of the stratiform region of a fast-moving squall line. Part I: General description and water and heat budgets [J]. J. Atmos. Sci., 1994, 51(14): 2046-2074.
[45] STEINER M, HOUZE R A (Jr.), YUTER S E. Climatological characterization of three-dimensional storm structure from operational radar and rain gauge data [J]. J. Appl. Meteor., 1995, 34(9): 1978-2007.
[46] TAO W K, LANG S, SIMPSON J, et al. Vertical profiles of latent heat release and their retrieval for TOGA COARE convective systems using a cloud resolving model, SSM/I, and ship-borne radar data [J]. J. Meteor. Soc. Japan, 2000, 78(4): 333-355.
[47] XU K M. Partitioning mass, heat, and moisture budgets of explicitly simulated cumulus ensembles into convective and stratiform components [J]. J. Atmos. Sci., 1995, 52(5): 551-573.
[48] LANG S, TAO W K, SIMPSON J, et al. Modeling of convective-stratiform precipitation processes: Sensitivity to partition methods [J]. J. Appl. Meteor., 2003, 42(4): 505-527.

Citation: XU Feng-wen, XU Xiao-feng, CUI Xiao-peng et al. Radiative and microphysical effects of ice clouds on a torrential rainfall event over Hunan, China. *J. Trop. Meteor.*, 2012, 18(3): 393-402.